Progress in Superconductivity Vol.3 No.1 pp5-12 31 October 2001

Evolution of the Vortex Melting Line with Irradiation Induced Defects

Wai-Kwong Kwok,[*], L. M. Paulius[+], Christophe Marcenat[++], R. J. Olsson[*], G. Karapetrov[*], A. Mazilu[*], V. Tobos[+] and G. W. Crabtree[*]

[*]*Materials Science Division, Argonne National Laboratory, Argonne, IL 60439, USA*

[+]*Dept of Physics, Western Michigan University, Kalamazoo, MI 49008, USA*

[++]*Commissariat A L'Energie Atomique, Grenoble, France.*

Received 10 September 2001

Abstract

Our experimental research focuses on manipulating pinning defects to alter the phase diagram of vortex matter, creating new vortex phases. Vortex matter offers a unique opportunity for creating and studying these novel phase transitions through precise control of thermal, pinning and elastic energies. The vortex melting transition in untwinned $YBa_2Cu_3O_{7-\delta}$ crystals is investigated in the presence of disorder induced by particle irradiation. We focus on the low disorder regime, where a glassy state and a lattice state can be realized in the same phase diagram. We follow the evolution of the first order vortex melting transition line into a continuous transition line as disorder is increased by irradiation. The transformation is marked by an upward shift in the lower critical point on the melting line. With columnar defects induced by heavy ion irradiation, we find a second order Bose glass transition line separating the vortex liquid from a Bose glass below the lower critical point. Furthermore, we find an upper threshold of columnar defect concentration beyond which the lower critical point and the first order melting line disappear together. With point defect clusters induced by proton irradiation, we find evidence for a continuous thermodynamic transition below the lower critical point.

Keywords : Vortex, phase transitions, melting, irradiation, defects

I. Introduction

The phase diagram of vortex matter in high temperature superconductors continues to intrigue us with discoveries of new phases and transitions. Recently, two new phase transitions have been reported: an inverse melting transition in $Ba_2Sr_2CaCu_2O_x$ [1] and a liquid-liquid transition in $YBa_2Cu_3O_{7-\delta}$ [2]. The vortex phase diagram of these materials is far from understood and offers a rich and complex area of study. The vortex phase diagram is determined by the interplay of four basic energies, thermal, elastic due to vortex-vortex interactions, inter-planar coupling, and pinning energy. The richness and complexity of vortex phase diagram arises from the wide range over which these parameters can be varied. For example, the inter-vortex spacing can be varied by several orders of magnitude simply by increasing the applied magnetic field from fractions of a Gauss to several Tesla. In contrast, the distance between lattice sites in atomic solids is much more difficult to vary. Changes in the inter-planar coupling enable vortices to appear as flexible lines which can become entangled, or as decoupled pancake vortices. Experimentally, the thermal, interaction, and pinning energies can be controlled in a straightforward manner simply by varying the temperature, the applied magnetic field, and by introducing defects through irradiation. In relatively pure samples of $Ba_2Sr_2CaCu_2O_x$ and $YBa_2Cu_3O_{7-\delta}$, it has been shown that the melting of the vortex lattice to a vortex liquid

occurs via a first order phase transition [3,4]. The introduction of relatively large amounts of disorder transforms the first order transition into an irreversibility line characterized by a second or higher order transition [5-7]. With careful control of the incremental introduction of defects, one can directly investigate one of the fundamental problem in the physics of phase transitions, namely the evolution of a first order phase transition into higher order with increasing disorder.

In this paper, we review the effect of disorder on the vortex phase diagram of optimally doped untwinned single crystals of $YBa_2Cu_3O_{7-d}$ (YBCO). Disorder is introduced via carefully controlled proton and high-energy heavy ion irradiation, whereby a specific number of point and correlated defects are created, respectively. We concentrate on the low defect density case where the first order vortex melting transition is not completely suppressed. We show that the lower critical point which indicates the termination of the first order melting transition at low fields [8, 9] mediates the suppression and transformation of the first order transition to higher order.

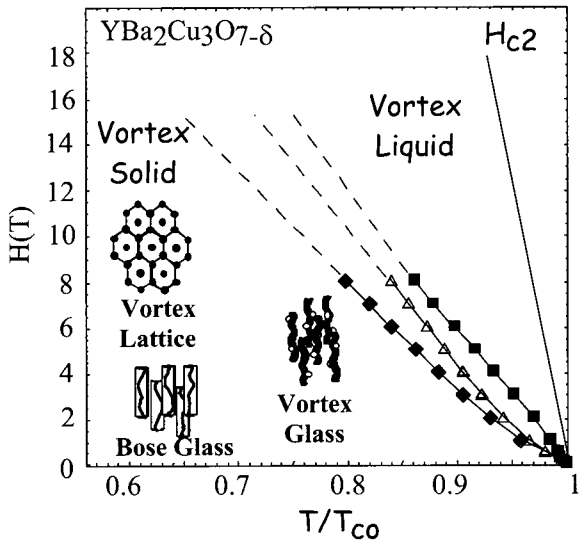

Fig. 1. Vortex phase diagram of $YBa_2Cu_3O_{7-\delta}$ showing the first order melting line before irradiation (triangles), and the irreversibility lines after proton (diamonds) and heavy ion (squares) irradiation.

II. Sample Preparation

Starting samples are high quality single crystals of $YBa_2Cu_3O_{7-d}$ grown using the self-flux technique [10] and subsequently annealed in flowing oxygen at 420° C for ten days. Twin boundaries are removed using a thermo-mechanical technique, resulting in optimally doped untwinned crystals which typically display zero field transition temperatures of T_{co}~93K. In the presence of a magnetic field, the tail of the superconducting resistive transition displays a sharp 'kink' associated with the first order vortex melting transition [11]. We further test for residual twin boundary pinning by performing angular dependent resistivity measurements searching for any vestige of anisotropic pinning [12]. These precharacterizations guarantee that the reference samples are of high quality and that any changes in their pinning behavior from irradiation can be attributed solely to the induced defects.

III. Irradiation

The pronounced effect of defects induced by proton and heavy ion irradiation on the vortex melting transition is demonstrated in Fig. 1. Proton irradiation is believed to create point defects and clusters of defects as large as 70Å in diameter [13], while high energy heavy ion irradiation creates amorphous columnar defects, whose diameter can range from about 60Å for gold ions [14] up to 130Å for uranium ions [15] and whose length can span the entire thickness of the sample. With heavy ions, the irradiation dose can be described by a dose matching field, defined so that the density of columnar defects coincides with the density of vortices. For example, a dose of 5 x 10^{11} ions/cm^2 corresponds to a dose matching field B_Φ=1T. Fig. 1 compares the first order melting line of an untwinned YBCO crystal with the irreversibility lines of two other crystals, irradiated with protons and heavy ions, respectively. Irradiation with 9MeV protons to a dose of 3 x 10^{16} p/cm^2 completely suppresses the first order transition. It is replaced by an irreversibility line which lies a few degrees below the melting transition. In this case, the vortex solid state could be a vortex glass [16, 7], though not all the glass hallmarks are seen, as we describe later. In contrast, with 1.4 GeV Pb-ion

irradiation to a dose matching field of B_Φ=1Tesla, the irreversibility line lies above the first order melting line. In this case, the solid state has been shown to be a Bose glass [17, 18].

IV. Columnar Defects

We investigate the intermediate regime between these transformations when only a small density of defects are present. Fig. 2 delineates the resistive transition at different values of the magnetic field directed along the crystallographic c-axis before and after irradiation of an untwinned crystal. The sharp kink in the resistivity associated with the first order vortex lattice to liquid transition before irradiation (thin lines) can be seen at all fields from 0.5T to 8T. After irradiation with 1.4GeV Pb ions to a dose matching field of B_Φ=500G, the 'kink' associated with the first order transition becomes suppressed at fields below 1.5T as shown by the temperature derivative of the resistivity (inset to Fig. 2). The absence of a sharp peak in the temperature derivative indicates the kink and associated first order melting do not occur. We define the lower critical point H_{lcp} as the lowest field where the first order melting transition is observed. Remarkably, H_{lcp}, can be systematically pushed to higher fields with increasing columnar defect density as shown in Fig. 3.

A careful inspection of the resistive transition for $H < H_{lcp}$ shows non-ohmic behavior above the zero resistance temperature. This is shown in Fig. 4, where the resistivity for H=0.5T||c is measured with two different current densities. The arrow indicates the onset of non-ohmic behavior which we define as the irreversibility temperature. In the presence of columnar defects, the vortex solid is predicted to be a Bose glass [17]. The voltage current behavior can be fitted to the scaling ansatz, $E_\perp \ell_\perp^{(1+z)} \sim F_\pm(\ell_\perp \ell_\| J_\perp\Phi_o/cT\ ,\ \ell_\perp H_\perp\Phi_o/4\pi T)$ where E, and J are the electric field and current density, respectively and $\ell_\perp \sim (T-T_{BG})^{-\nu}$ and $\ell_\| \sim \ell_\perp^2$ are the two anisotropic correlation lengths. At $T=T_{BG}$, $E \sim J^{(z+1)/3}$ where z is the dynamic exponent related to the fluctuation relaxation timescale, $t \sim \ell_\perp^z$. We can collapse the E-J curves into two curves as shown in Fig. 5 and obtain critical exponents of $\nu=1.2 \pm 0.1$ and $z=4 \pm 0.1$. These exponents are comparable to those

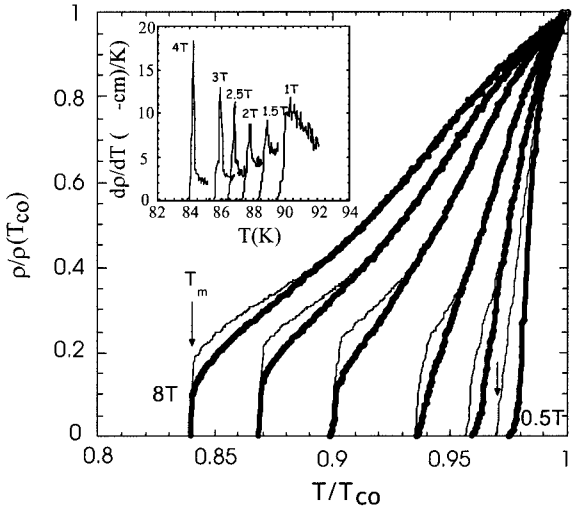

Fig. 2. Temperature dependence of the resistivity before (thin lines) and after (thick lines) irradiation with 1.4GeV Pb ions to B_Φ=500G, in magnetic fields of H=0.5, 1, 2, 4, 6, and 8T || c. Inset shows the temperature derivative of the resistivity at intermediate and low fields for the irradiated sample.

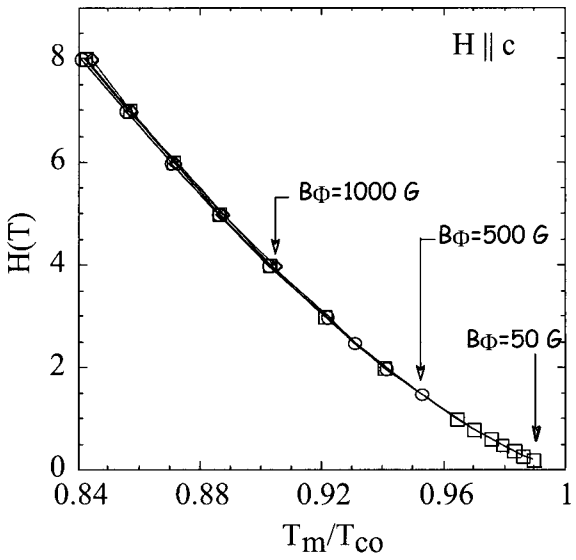

Fig. 3. Vortex phase diagram showing the systematic shift of the lower critical point (shown by arrows) in samples irradiated with 1.4GeV Pb-ions to a matching field of B_Φ=50G, 500G and 1000G.

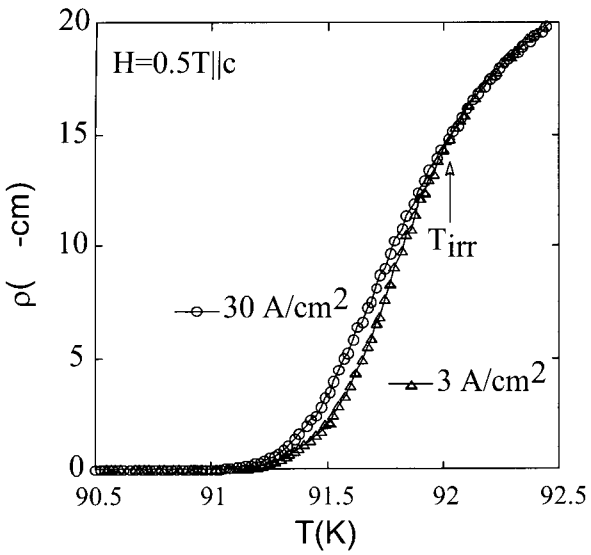

Fig. 4. Temperature dependence of the resistivity for H=0.5T measured with two different current densities.

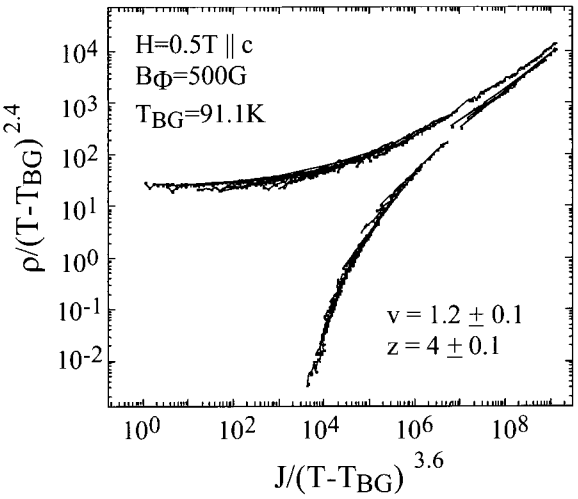

Fig. 5. Scaling of the E-J curves with the Bose glass ansatz.

obtained in untwinned crystals irradiated with a much higher dose of B_Φ=1T [18] where the first order transition is completely suppressed at all fields. A plot of the normalized irreversibility temperature as a function of angle for $H < H_{lcp}$ shows a sharp cusp near $\theta=0^\circ$ when the magnetic field is aligned with the columnar defects, another hallmark of the Bose glass transition. The magnitude of the $T_{irr}(\theta)$ cusp near

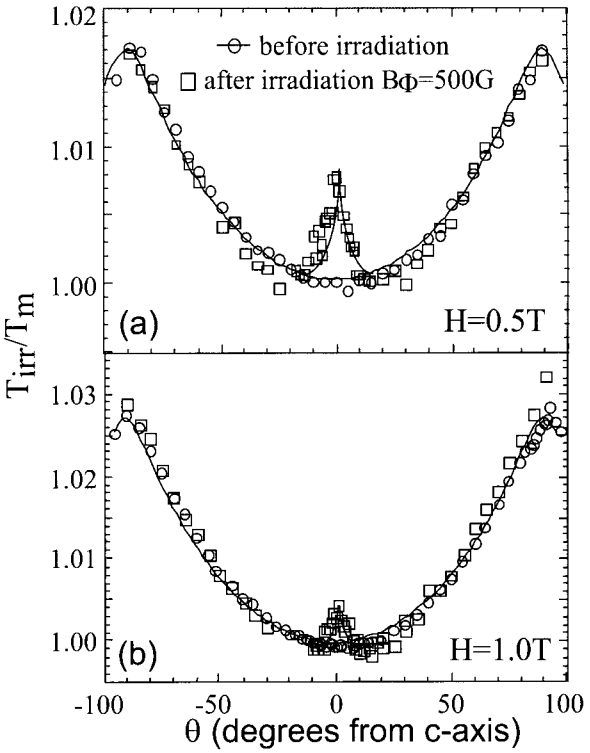

Fig. 6. Angular dependence of the normalized irreversibility temperature for H=0.5T and 1.0T.

$\theta=0^\circ$ decreases as the field is increased towards H_{lcp} as shown in Fig. 6. Our results demonstrate that the Bose glass melting line merges smoothly with the first order vortex lattice melting line at the lower critical point as shown in Fig. 7 for a crystal irradiated with a dose matching field of B_Φ=500G.

The transition from a Bose glass state to a vortex lattice state with increasing magnetic field suggests a transformation of the vortex structure near the lower critical point. A simple energy argument suggests that the cross-over from the glassy state to the lattice state will occur when the vortex elastic energy becomes greater than the vortex pinning energy. We estimate the vortex elastic energy as $E_{el}=\gamma\varepsilon_o u^2/a_o$ where γ is anisotropy, $\varepsilon_o=(\Phi_o/4\pi\lambda)^2$, $a_o\sim(\Phi_o/B)^{1/2}$ and u is the average displacement from the vortex equilibrium position. The pinning due to columnar defects can be estimated as some fraction of the characteristic vortex energy, $E_{pin} \sim B_\Phi/B(\gamma\varepsilon_o a_o)$. [19] We use the Lindemann expression for the average vortex displacement $u^2=c_L^2 a_o^2$ along the vortex

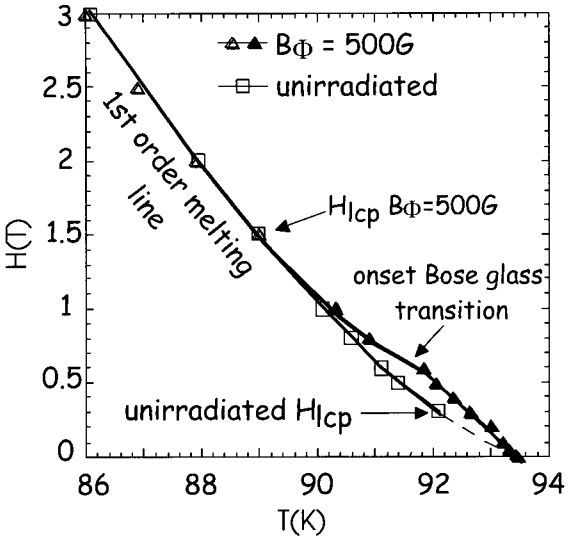

Fig. 7. Vortex phase diagram of unirradiated and irradiated untwinned YBCO crystal.

melting line. At the lower critical point, $E_{el}=E_{pin}$. Thus the Lindemann criteria can be expressed as $c_L=(B_\Phi/B_{lcp})^2$, resulting in a simple expression which relates the Lindemann criteria to the dose matching field and the magnetic field. Substituting our results for B_Φ=2000G (B_{lcp}=5T), B_Φ=1000G (4T) and B_Φ=500G (1.5T) yields a very reasonable Lindemann criteria of $c_L=0.18 \pm 0.02$.

Recently, we have observed that the lower critical point does not extend beyond B_{lcp}=5T. An irradiation dose of B_Φ=3500G is sufficient to completely suppress the first order vortex melting transition at all fields, replacing it with a Bose glass transition. This suggests a threshold value for defect concentration above which the first order transition suddenly disappears. This does not support the notion that a first order melting transition transforms *smoothly* into a higher order continuous transition with increasing defect density. [20]. Our results show that the first order transition transforms into a continuous transition through a shift in the lower critical point.

V. Point Defects

The lower critical point also plays a similar role in untwinned YBCO crystals irradiated with 9MeV protons. Fig. 8 shows the temperature dependent

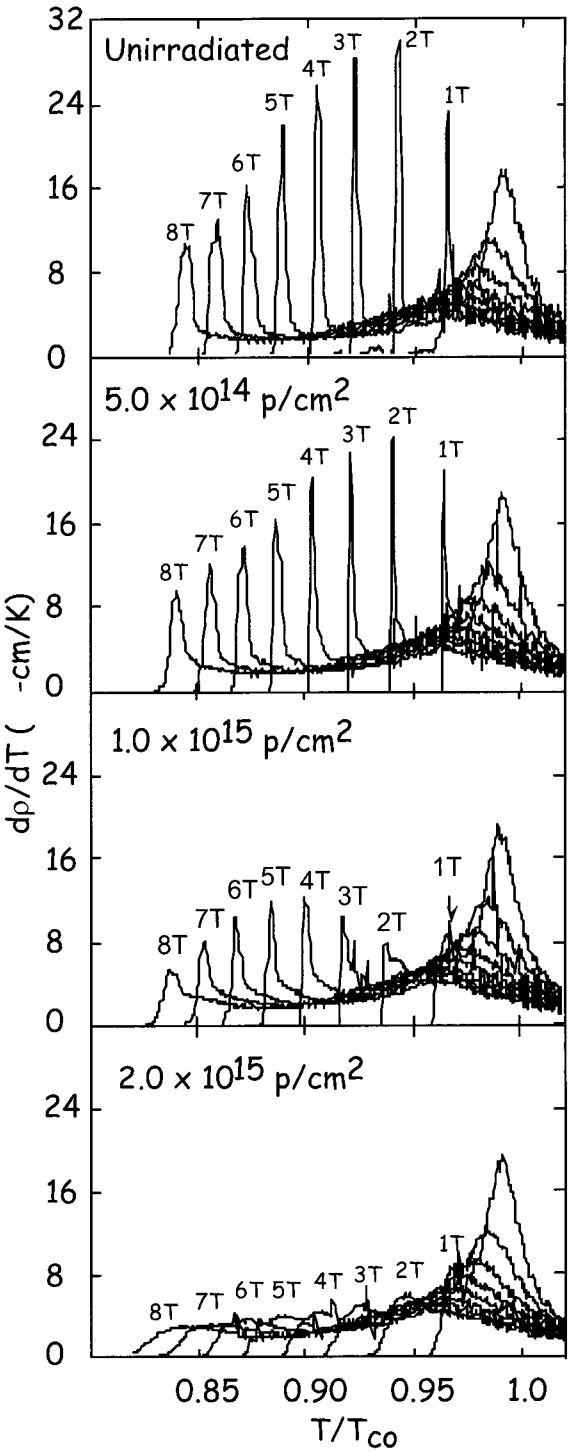

Fig. 8. Temperature derivative of the superconductive resistive transition of an untwinned YBCO crystal irradiated with subsequent doses of 9.0 MeV protons.

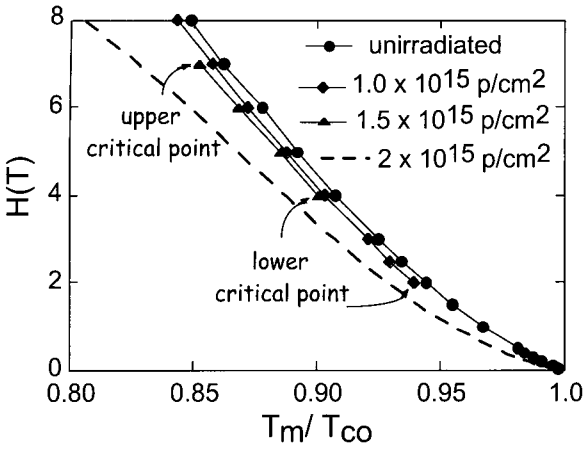

Fig. 9. Vortex phase diagram of untwinned YBCO irradiated with 9 MeV protons.

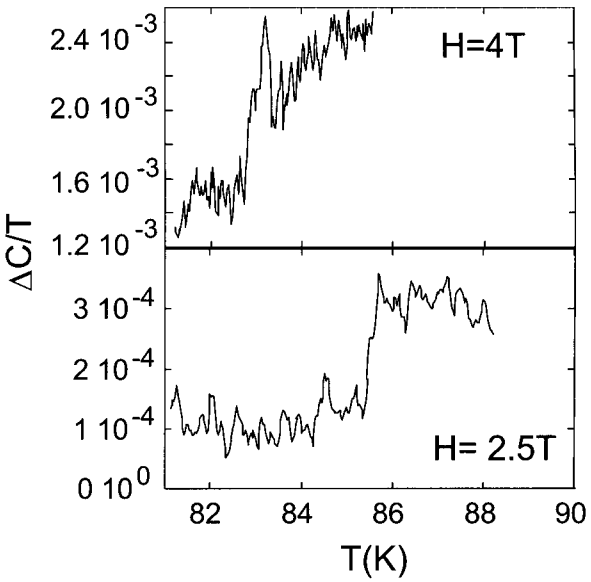

Fig. 10. Differential heat capacity measurements above and below the lower critical point (H_{lcp}=3T) of an untwinned YBCO crystal irradiated with 1.0 x 10^{15} protons/cm^2

superconducting resistive transition for a single untwinned YBCO crystal which was irradiated with increasing subsequent doses of protons up to 2 x 10^{15} protons/cm^2. Note the disappearance of the peak in the derivative associated with the first order transition at low and high magnetic fields. The vortex phase diagram derived from transport measurements is shown in Fig. 9. The lower critical point shifts from below 0.05T in the unirradiated sample, to H_{lcp}=2T to 4T by increasing the irradiation dose from 1.0 x 10^{15} p/cm^2 to 1.5 x 10^{15} p/cm^2, respectively. A dose of 2 x 10^{15} p/cm^2 completely suppresses the vortex lattice to liquid first order phase transition. At much higher doses of 3 x 10^{16} p/cm^2 we have shown that a vortex glass transition may exist.[7] There is also a downward shift in temperature of the transition lines with subsequent proton irradiation, in contrast to the upward shift observed in crystals irradiated with high energy heavy ions as demonstrated in Fig. 1 and 7.

The solid state below the lower critical point in proton irradiated samples could be a vortex glass state induced by cluster defect formation [for further discussion see ref. 9]. However, voltage-current measurements have so far yielded only ohmic behavior, unlike the I-V scaling behavior shown in Fig. 5 for columnar defected samples and expected for the vortex glass. However, a scaling of the ohmic resistivity data for the sample irradiated with 3 x 10^{16} protons/cm^2 has yielded a field independent scaling exponent consistent with a vortex glass transition [7]. More recently, we have observed a change in the specific heat behavior above and below the lower critical point in another untwinned YBCO crystal irradiated with 1.0 x 10^{15} p/cm^2. Above H_{lcp}=3T, the differential heat capacity displays a peak associated with a first order phase transition, while below H_{lcp}, it shows a step associated with a continuous phase transition as shown in Fig. 10. The observation of a thermodynamic phase transition in proton irradiated YBCO below the lower critical point gives further credence to a vortex glass state at low fields / high temperatures.

VI. Conclusion

In summary, the lower critical point plays an important role in the transformation of the first order vortex melting line into a continuous transition line. In both the heavy ion and proton irradiated samples, the evolution from a first order to continuous transition occurs through an upward shift of the lower critical point. In the case of columnar defects, the phase transition line below the lower critical point is a Bose glass transition. In the case of point defects,

we demonstrate a clear continuous thermodynamic phase transition below the lower critical point, possibly related to a vortex glass transition. Our studies show that the careful manipulation of the vortex elastic, pinning, and thermal energies leads to new transitions and phases, demonstrating that vortex matter can serve as an ideal platform for the study of phase transitions.

Acknowledgments

This work is supported by the U.S. DOE, BES--Materials Science, contract #W-31-109-ENG-38 (WWK, RJO, GK, AM, GWC) and by the NSF grant DMR-0072880 (LMP, VT).

References

[1] N. Avraham, B. Khaykovich, Y. Myasoedov, M. Rappaport, H. Shtrikman, D. E. Feldman, T. Tamegai, et al., "Inverse melting of a vortex lattice", Nature 411, 451-454 (2001).

[2] F. Bouquet, C. Marcenat, E. Steep, R. Calemczuk, W. K. Kwok, U. Welp, G. W. Crabtree, R. A. Fisher, N. E. Phillips, et al., "An unusual phase transition to a second liquid vortex phase in the superconductor $YBa_2Cu_3O_7$", Nature 411, 448-451 (2001).

[3] E. Zeldov et al., Nature (London) 375, 373 (1995); H. Pastoriza, M. F. Goffman, A. Arribére, and F. de la Cruz, "First order phase transition at the irreversibility line of $Bi_2Sr_2CaCu_2O_8$", Phys. Rev. Lett. 72, 2951-2954 (1994).

[4] U. Welp, J. A. Fendrich, W. K. Kwok, G. W. Crabtree, and B. W. Veal, "Thermodynamic evidence for a flux line lattice melting transition in $YBa_2Cu_3O_{7-\delta}$", Phys. Rev. Lett. 76, 4809-4812 (1996); R. Liang, D. A. Bonn, and W. N. Hardy, "Discontinuity of reversible magnetization in untwinned YBCO single crystals at the first order vortex melting transition", Phys.Rev. Lett. 76, 835-838 (1996).

[5] W. K. Kwok, L. M. Paulius, V. M. Vinokur, A. M. Petrean, R. M. Ronningen, and G. W. Crabtree, "Vortex pinning of anisotropically splayed defects in $YBa_2Cu_3O_{7-\delta}$", Phys. Rev. Lett. 80, 600-603 (1998)

[6] L. M. Paulius, J. A. Fendrich, W.-K. Kwok, A. E. Koshelev, V. M. Vinokur, G. W. Crabtree and B. G. Glagola, "Effects of 1-GeV uranium ion irradiation on vortex pinning in single crystals of the high-temperature superconductor $YBa_2Cu_3O_{7-\delta}$", Phys. Rev. B 56, 913-924 (1997).

[7] A. M. Petrean, L. M. Paulius, W.-K. Kwok, J. A. Fendrich,* and G.W. Crabtree, "Experimental evidence for the vortex glass phase in untwinned, proton irradiated $YBa_2Cu_3O_{7-\delta}$", Phys.Rev. Lett. 84, 5852-5855 (2000)

[8] W. K. Kwok, R. J. Olsson, G. Karapetrov, L. M. Paulius, W. G. Moulton, D. J. Hofman, and G.W. Crabtree, "Critical points in heavy ion irradiated untwinned $YBa_2Cu_3O_{7-\delta}$ crystals", Phys. Rev. Lett 84, 3706-3709 (2000).

[9] L. M. Paulius, W.-K. Kwok, R. J. Olsson, A. M. Petrean, V. Tobos, J. A. Fendrich, G. W. Crabtree, C. A. Burns and S. Ferguson, "Evolution of the vortex phase diagram in $YBa_2Cu_3O_{7-\delta}$ with random point disorder", Phys. Rev. B 61, R11910-R11913 (2000).

[10] D. L. Kaiser, F. Holtzberg, B. A. Scott, and T. R. McGuire, "Growth of $YBa_2Cu_3O_x$ single crystals", Appl. Phys. Lett. 51, 1040-1042 (1987).

[11] J. A. Fendrich, U. Welp, W. K. Kwok, A. E. Koshelev, G. W. Crabtree, and B. W. Veal, "Static and dynamic vortex phases in $YBa_2Cu_3O_{7-\delta}$", Phys. Rev. Lett. 77, 2073-2076 (1996).

[12] W. K. Kwok, U. Welp, G. W. Crabtree, K. G. Vandervoort, R. Hulscher, and J. Z. Liu, "Direct observation of dissipative flux motion and pinning by twin boundaries in $YBa_2Cu_3O_{7-\delta}$ single crystals", Phys. Rev. Lett. 64, 966-969 (1990).

[13] M. A. Kirk and H. W. Weber, in Studies of High Temperature Superconductors, edited by A. Narlikar ~Nova Science Publishers,Commack, NY, 1992!, Vol. 10, p. 243.

[14] L. Civale, A. D. Marwick, T. K. Worthington, M. A. Kirk, J. R. Thompson, L. Krusin-Elbaum, Y. Sun, J. R. Clem, and F. Holtzberg, "Vortex confinement by columnar defects in $YBa_2Cu_3O_7$ crystals: enhanced pinning at high fields and temperatures", Phys.Rev. Lett. 67, 648-651 (1991).

[15] from Scanning Tunneling Microscopy studies by M. Iavarone and G. Karapetrov (unpublishcd)

[16] M. P. A. Fisher, "Vortex-glass superconductivity: a possible new phase in bulk high-T_c oxides", Phys. Rev. Lett. 62, 1415-1418 (1989); D. S. Fisher, M. P.A. Fisher, and D. A. Huse, "Thermal fluctuations, quenched disorder, phase transitions, and transport in type-II superconductors", Phys. Rev. B 43,130-159 (1991).

[17] D. R. Nelson and V. M. Vinokur, "Boson locatization and pinning by correlated disorder in high-temperature superconductors", Phys. Rev. Lett. 68, 2398-2401 (1992); ibid., "Boson localization and correlated pinning of superconducting vortex arrays", Phys. Rev. B 48, 13 060-13097 (1993); ibid., "Bose glass scaling for superconducting vortex arrays revisited", Phys. Rev. B61, 5917-5919 (2000).

[18] R. J. Olsson, W. K. Kwok, L.M. Paulius, A. M. Petrean, D. J. Hofman and G. W. Crabtree, "The Bose glass transition in columnar defected untwinned $YBa_2Cu_3O_{7-\delta}$", (unpublished).

[19] V. Vinokur, B. Khaykovich, E. Zeldov, M. Konczykowski, R.A. Doyle, and P.H. Kes, "Lindemann criterion and vortex-matter phase transitions in high-temperature superconductors", Physica C 295, 209-217, (1998).

[20] Y. Imry and M. Wortis, "Influence of quenched impurities on first-order phase transitions", Phys. Rev. B 19, 3580-3585 (1979).